Kinetics and Catalysis, Vol. 43, No. 1, 2002, pp. 129–138. Translated from Kinetika i Kataliz, Vol. 43, No. 1, 2002, pp. 140–149.

Physicochemical and Catalytic Properties of $La_{1-x}Ca_xFeO_{3-0.5x}$ Perovskites Prepared Using Mechanochemical Activation

L. A. Isupova, S. V. Tsybulya, G. N. Kryukova, G. M. Alikina, N. N. Boldyreva, A. A. Vlasov, O. I. Snegurenko, V. P. Ivanov, V. N. Kolomiichuk, and V. A. Sadykov

Boreskov Institute of Catalysis, Siberian Division, Russian Academy of Sciences, Novosibirsk, 630090 Russia

Received March 29, 2000

Abstract—The phase composition of $La_{1-x}Ca_xFeO_{3-0.5x}$ perovskites synthesized from preactivated oxides was studied by powder X-ray diffraction analysis and differential dissolution. The system does not form a continuous series of homogeneous solid solutions. No intermediate samples from this series are monophasic. It was found that the synthesis under nonequilibrium conditions (mechanical activation + calcination at 900°C for 4 h) resulted in nonequilibrium microheterogeneous solid solutions with degrees of calcium substitution for lanthanum of no higher than 0.5. A longer calcination (for 16 h) or an increase in the calcination temperature of solutions up to 1100 °C decreased the calcium content of the samples down to $x \sim 0.2$ because of the formation of a brownmillerite phase. The catalytic activity of the test samples in the oxidation of CO changed nonmonotonically with x, and it was maximum at $x = 0.5$–0.6, which correlates with the maximum density of interphase boundaries in these samples.

INTRODUCTION

The defect structure of perovskites, oxides with the general formula $A^1_{1-x}A^2_xBO_{3-y}$ (A^1 = La, …; A^2 = Ca, Sr, Ba…; B = Mn, Co, Fe…), is a factor responsible for their catalytic activity in various deep oxidation reactions. It is believed that the introduction of an alkaline-earth cation into a lanthanum sublattice results in either or both the appearance of vacancies in the lanthanum sublattice and an increase in the charge on transition-metal cations [1–3]. In the test series of $La_{1-x}Ca_xFeO_{3-0.5x}$ perovskites, the substitution of calcium for lanthanum results in the appearance of oxygen vacancies because the Fe^{4+} cation is unstable [2]. According to Wu *et al.* [3], weakly bound oxygen can be adsorbed on vacancies; consequently, the catalytic activity is proportional to the fraction of introduced calcium.

However, our previous studies on the specific catalytic activity in the $La_{1-x}Ca_xFeO_{3-0.5x}$ system synthesized from oxides by a ceramic process demonstrated that the activity as a function of the chemical composition exhibits a maximum [4]. In this case, it was found that the system forms a limited series of calcium solutions in a perovskite structure at $x \le 0.17$ rather than a continuous series of homogeneous solid solutions [4]. The members of a homologous series (vacancy-ordered phases) with the general formula $A_nB_nO_{3n-1}$ (A = La, Ca; B = Fe), where $n = 2$ or 3, are formed in the compositions with $x > 0.5$ [5]. The members of the homologous series are characterized by different sequences of alternating octahedral (O) and tetrahedral (T) layers depending on n. Brownmillerite ($Ca_2Fe_2O_5$, a member of the homologous series with $n = 2$) is characterized by the sequence OTOTOT…, and the Grenier phase ($La_{0.33}Ca_{0.67}FeO_{2.67}$ with $n = 3$) is characterized by the sequence OOTOOT…[5]. However, a sample of the composition $La_{0.5}Ca_{0.5}FeO_{2.75}$ with $x = 0.5$ is not a member of the homologous series with $n = 4$ and the characteristic sequence OOOTOOOTOOOT…. According to high-resolution electron-microscopic data, this sample consists of a microheterogeneous solid solution [4, 6]. As found previously [4], a maximum activity in the reaction of carbon monoxide oxidation for a sample with $x = 0.5$ can result from the morphology or microstructure of its particles, namely, the occurrence of coherent grain boundaries. Coordinatively unsaturated clustered adsorption centers can be formed at the outlet of these boundaries on the surface [6].

The procedure used for preparing oxides also has a considerable effect on the defect structure and microstructure [7]. This effect was most pronounced in syntheses under nonequilibrium conditions, such as mechanochemical, plasmo-chemical, cryochemical, and explosion syntheses. These methods find expanding applications, in particular, in the preparation of catalysts.

Perovskites can be synthesized by a mechanochemical method at lower temperatures and shorter calcination times as compared with those used in a ceramic method [8]. Under these conditions, the ordering of oxygen vacancies can be hindered. It is likely that this provides an opportunity to prepare a continuous series of the solid solutions of calcium in a lanthanum ferrite structure and to follow the effect of point defects on the catalytic activity of perovskites from this series.

0023-1584/02/4301-0129$27.00 © 2002 MAIK “Nauka / Interperiodica”

The aim of this study was to examine the synthesis of homogeneous solid solutions in the $La_{1-x}Ca_xFeO_{3-0.5x}$ system with the use of mechanochemical activation, to analyze the real structure of the samples, and to evaluate the catalytic activity in a model reaction of carbon monoxide oxidation.

EXPERIMENTAL

Catalysts. The samples of $La_{1-x}Ca_xFeO_{3-0.5x}$ ($x = 0$, 0.2, 0.4, 0.6, 0.8, and 1) were prepared by the calcination of mechanically activated mixtures of parent oxides taken in appropriate ratios at 700–1100°C for 4 h. The activation was performed in an APF-5 water-cooled centrifugal planetary ball mill at an acceleration of 40 *g* for 6 min. The weight ratio between the activated powder and steel grinding balls was 1 : 8. The time of activation for ternary mixtures was chosen based on previous data on the formation of crystalline products at the stage of activation of binary mixtures (iron oxide and lanthanum oxide or iron oxide and calcium oxide); these crystalline products are lanthanum ferrite and calcium ferrite, respectively [9, 10]. The following starting reagents were used: La_2O_3 prepared from chemically pure $La(NO_3)_2$ by calcination at 500°C for 4 to 5 h, chemically pure Fe_2O_3, and chemically pure CaO.

Investigation techniques. The prepared samples were examined by powder X-ray diffraction analysis, differential dissolution, high-resolution electron microscopy, and secondary-ion mass spectrometry. The specific surface areas and catalytic activities of the samples were also determined.

The X-ray diffraction analysis was performed on an URD-6 diffractometer using CuK_α radiation. Survey X-ray diffraction patterns were recorded on chart paper at a velocity of 1 deg/min in the range of 2θ angles of 10°–70°. To refine the phase composition (the occurrence of phases in small amounts or vacancy-ordered phases, which are determined by weak superstructure reflections), the X-ray diffraction patterns were scanned at a step of $2\theta = 0.02°$ and an acquisition time of 30 s in each point.

The quantitative phase analysis and the determination of the stoichiometry of the resulting phases were performed by differential phase dissolution. This more accurate method makes it possible to analyze phases that occur in low concentrations (lower than 5%) or phases in an X-ray amorphous state [11]. The method is based on separating the solubility regions of various phases under varied dissolution conditions (temperature and acidity of solution). The temperature of the solution was increased from room temperature to 90°C. The samples were dissolved using HCl solutions with concentrations ranging from 1 to 10 N. The solution components were analyzed by inductively coupled plasma atomic emission spectrometry. Photometric measurements were performed on a BAIRD instrument (the Netherlands).

The high-resolution electron-microscopic data were obtained on a JEM-2010 instrument with a resolution of 1.4 Å.

The specific surface area was determined by the BET method from the thermal desorption of argon at 300°C.

The secondary-ion mass-spectrometric measurements were performed on an MS-7201 mass spectrometer. The surface and bulk compositions of the samples were analyzed. The energy of argon ions was 4 keV, and the beam current density was 60 μA/cm^2. The samples were supported on an indium foil to prevent charging in the course of bombardment. The secondary-ion currents of La^+, Ca^+, and Fe^+ were experimentally determined as functions of the exposure time. Data on the surface composition were obtained after treatment for 66 s; this time was required for the removal of adsorbed gases. Data on the bulk composition were obtained after treatment for 1000 s, when the steady-state ion currents were attained. At an etching rate of 5 Å/min, the above values corresponded to the thickness of sputtered layers of ~5 and 100 Å, respectively. The relative experimental error was no higher than 20%.

The small-angle X-ray scattering (SAXS) data were obtained with the use of CuK_α radiation, a nickel filter, and an amplitude analyzer. An analysis of the integral intensity of small-angle scattering was used for determining the relative density of extended defects [12, 13].

The catalytic activity was determined in a model reaction of CO oxidation at 400, 450, and 500°C in a batch-flow reactor using a catalyst fraction with a particle size of 1 to 2 mm. The products were analyzed by chromatography. The sample weight was 1 g; the circulation rate was 1200 l/h; and the feed rate of the reaction mixture (1% CO + 1% O_2 in He) was 10 l/h. The samples were pretreated in a flow of the reaction mixture at 500°C for 0.5–1 h. The determination error in the concentrations of initial components and products was no higher than 20%.

RESULTS AND DISCUSSION

Phase Composition

According to X-ray diffraction data, the phases of perovskite (for $x = 0$–0.8), brownmillerite (for $x = 0.6$–1), and parent oxides ($x = 0$–1) were detected in the samples calcined at 700°C (Table 1). An increase in the calcination temperature to 900 or 1100°C (Tables 2, 3) only resulted in a considerable decrease in the parent oxide concentrations. The data are indicative of a widening of the region of formation of homogeneous solid solutions in the system up to a composition with $x = 0.4$ (Fig. 1a, spectrum *3*), as compared with the samples of a ceramic series [4]. Indeed, the main peaks of perovskite observed in the spectrum of a $La_{0.6}Ca_{0.4}FeO_{2.8}$ sample exhibited lower intensities, and they were shifted and broadened with respect to the peaks of lanthanum ferrite (Fig. 1a, spectrum *1*). This fact is indicative of

Table 1. Chemical analysis of the samples (calcination temperature of 700°C; 4 h)

Sample*, (S_{sp}, m^2/g)	Formula according to chemical analysis**	Phase composition according to XRD data	Phase contents according to differential dissolution***, %
$LaFeO_3$ (8.7)	La_1Fe_1	$LaFeO_3$ Fe_2O_3 La_2O_3	La_1Fe_1—73 Fe—1.8 La—25.2
$La_{0.8}Ca_{0.2}FeO_{2.9}$ (8.4)	$La_{0.84}Ca_{0.2}Fe_1$	Perovskite Fe_2O_3 La_2O_3	$La_1Fe_1 + Ca_1Fe_1$—60 Fe—6.4 La—32.9 Ca—0.7
$La_{0.6}Ca_{0.4}FeO_{2.8}$ (4.4)	$La_{0.65}Ca_{0.38}Fe_1$	Perovskite Fe_2O_3 La_2O_3	$La_1Fe_1 + Ca_1Fe_1$—60 Fe—6.9 La—33.1
$La_{0.4}Ca_{0.6}FeO_{2.7}$ (4.6)	$La_{0.48}Ca_{0.5}Fe_1$	Perovskite Fe_2O_3 La_2O_3 CaO	$La_1Fe_1 + Ca_1Fe_1$—61.4 Fe—5.39 La—18.27 Ca—14.94
$La_{0.2}Ca_{0.8}FeO_{2.6}$ (3.3)	$La_{0.23}Ca_{0.73}Fe_1$	Perovskite $Ca_2Fe_2O_5$	$La_1Fe_1 + Ca_1Fe_1$—50
		Fe_2O_3 CaO	Fe—27.3 Ca—22.7
$Ca_2Fe_2O_5$ (3)	Ca_1Fe_1	$Ca_2Fe_2O_5$ CaO Fe_2O_3	Ca_1Fe_1—83 Ca—10 Fe—7

* The chemical formulas of the samples are indicated in accordance with the chosen stoichiometry of cations and the requirement of electric neutrality.

** The stoichiometric ratios between cations in the samples are given in accordance with the chemical analysis data upon complete dissolution of the samples.

*** The stoichiometric ratios between cations in the separated oxide phases and the percent concentrations of phases are given in accordance with the data of differential dissolution.

the inclusion of calcium into a perovskite structure. It was difficult to recognize a brownmillerite phase because the peak intensities of perovskite (Fig. 1a, spectrum *3*) and brownmillerite (Fig. 1a, spectrum *2*) are considerably different at similar peak positions. Because of this, the $La_{0.6}Ca_{0.4}FeO_{2.8}$ sample was additionally scanned over the region of small angles (Fig. 1b, spectrum *1*). The results provided support for the formation of a homogeneous solid solution because peaks at 7.37 and 5.24 Å typical of the brownmillerite structure were absent from the region of small angles (for example, these peaks are clearly pronounced in a $La_{0.2}Ca_{0.8}FeO_{2.6}$ sample (JCPDS 19-222)). A peak at 11.35 Å typical of the Grenier phase (JCPDS 30-260) was also not detected.

To refine the stoichiometric composition of the formed solid solutions and the phase composition, the samples were analyzed by differential dissolution [11]. Previously, we used this method for the analysis of samples from this series prepared by a ceramic process [4]. Tables 1–3 summarize data on the differential dissolution of all of the test samples depending on the temperature of calcination. The phase composition of each sample is considered below.

$LaFeO_3$. It was found that lanthanum ferrite was formed even at the stage of activation [8, 10]. An increase in the temperature of the subsequent calcination resulted in an increase in the product phase content (Tables 1–3) and in an improvement in the structure of the product [10]. Note that, after the calcination of a preactivated mixture at 900°C for 4 h, the amount of the product formed (~87%, Table 2) was equal to that in the ceramic synthesis after calcination for 150 h (87%) [4]. The conversion was as high as 95% after the calcination of an activated mixture at 1100°C for 4 h (Table 3).

$La_{0.8}Ca_{0.2}FeO_{2.9}$. The X-ray diffraction patterns of the samples calcined at 700°C suggest the occurrence of parent oxide phases and a phase with the perovskite structure. An increase in the calcination temperature up to 1100°C resulted in the almost complete disappearance of parent oxide phases.

A study of the stoichiometric composition of the phases by differential dissolution demonstrated that this multiphase system consists of La–Ca–Fe–O, Ca–Fe–O, and parent oxide phases. A special feature of the samples calcined at 700°C is that a La–Ca–Fe–O phase of a definite composition cannot be recognized in them because the relative calcium content of a solution decreases as the sample undergoes dissolution. Based

Table 2. Chemical analysis of the samples (calcination temperature of 900°C; 4 h)

Sample* (S_{sp}, m^2/g)	Formula according to chemical analysis**	Phase composition according to XRD data	Phase contents according to differential dissolution***, %
$LaFeO_3$ (3.3)	$La_{1.08}Fe_1$	$LaFeO_3$ Fe_2O_3 La_2O_3	La_1Fe_1—87.44 Fe—1.56 La—11
$La_{0.8}Ca_{0.2}FeO_{2.9}$ (3.1)	$La_{0.86}Ca_{0.22}Fe_1$	Perovskite Fe_2O_3 La_2O_3	$La_1Ca_{0.11}Fe_1$—72.5 Fe—5.5 La—16 Ca—1.1 Ca_1Fe_1—4.9
$La_{0.6}Ca_{0.4}FeO_{2.8}$ (2.1)	$La_{0.68}Ca_{0.38}Fe_1$	Perovskite Fe_2O_3 La_2O_3	$La_{0.78}Ca_{0.25}Fe_1$—81.3 Ca_1Fe_1—10.7 Fe—1.9 La—6.1
$La_{0.4}Ca_{0.6}FeO_{2.7}$ (1.9)	$La_{0.44}Ca_{0.59}Fe_1$	Perovskite $Ca_2Fe_2O_5$ Fe_2O_3 La_2O_3	$La_{0.78}Ca_{0.27}Fe_1$—47 Ca_1Fe_1—33 Fe—7.3 La—9.4 Ca—3.3
$La_{0.2}Ca_{0.8}FeO_{2.6}$ (1.7)	$La_{0.2}Ca_{0.8}Fe_1$	Perovskite $Ca_2Fe_2O_5$	$La_{0.67}Ca_{0.34}Fe_1$—32.9 Ca_1Fe_1—57.8 Fe—3.1 La—4 Ca—2.2
$Ca_2Fe_2O_5$ (0.9)	Ca_1Fe_1	$Ca_2Fe_2O_5$	Ca_1Fe_1—95 Ca—4 Fe—1

Note: Specific notes are given in Table 1.

on differential dissolution data, we suggested that the product particles consist of the following components: (a) a conglomerate of La–Fe–O and Ca–Fe–O phases with the particle surface enriched in a Ca–Fe–O oxide phase (the enrichment of the surface in calcium and iron cations was supported by SIMS data given below); (b) a layer of a La–Ca–Fe–O phase with a decreasing calcium content; and (c) a core that consists of a La–Fe–O phase. According to differential dissolution data, the amount of parent oxide phases decreased, the amount of calcium in a La–Ca–Fe–O phase increased, and the concentration of a Ca–Fe–O phase decreased as the calcination temperature was increased (Tables 1–3). The absence of brownmillerite peaks from the X-ray diffraction patterns of the samples can be explained by the fact that, according to differential dissolution data, the concentration of a Ca–Fe–O phase in the products was no higher than 5%.

$La_{0.6}Ca_{0.4}FeO_{2.8}$. According to X-ray diffraction data, perovskite and parent oxide phases occurred in the product calcined at 700°C. The phases of parent oxides disappeared, and the amount of a perovskite phase increased as the temperature of calcination was increased. According to differential dissolution data, as in the above case, a complex oxide phase of a definite stoichiometric composition cannot be recognized in the sample calcined at 700°C because of a considerable overlap between the solubility regions of lanthanum ferrite and calcium ferrite. An increase in the calcination temperature up to 900°C resulted in a decrease in the concentrations of parent oxide phases. In this case, a La–Ca–Fe–O oxide phase with a calcium content up to 0.25 mole fractions and a Ca–Fe–O phase can be recognized. According to differential dissolution data, the following two oxide phases are recognized after the calcination of the samples at 1100°C (Table 3): La–Ca–Fe–O with a calcium content of 0.2 mole fractions and a lanthanum-doped Ca–Fe–O phase containing superstoichiometric calcium.

$La_{0.4}Ca_{0.6}FeO_{2.7}$. The behavior of a sample with the specified stoichiometry was completely analogous to that of the foregoing sample. According to differential dissolution data, in the sample calcined at 900°C, the calcium content of the ternary oxide was 0.27 mole fractions (Table 2), and it decreased to 0.17 mole fractions after calcination at 1100°C.

$La_{0.2}Ca_{0.8}FeO_{2.6}$. According to X-ray diffraction data, perovskite, brownmillerite, and iron oxide phases were detected in the samples after calcination at 700°C. According to differential dissolution data, the stoichiometric composition of a perovskite phase after calcination at 900°C corresponded to $x = 0.34$. After calcina-

Table 3. Chemical analysis of the samples (calcination temperature of 1100°C; 4 h)

Sample* (S_{sp}, m^2/g)	Formula La : Ca : Fe according to chemical analysis**	Phase composition according to XRD data	Phase contents (%) and the La : Ca : Fe ratio according to differential dissolution***, %
$LaFeO_3$ (1.5)	$La_{1.03}Fe_1$	$LaFeO_3$ La_2O_3—traces	$La_{1.4}Fe_1$—95 La—5
$La_{0.8}Ca_{0.2}FeO_{2.9}$ (0.7)	$La_{0.84}Ca_{0.19}Fe_1$	Perovskite Fe_2O_3—traces La_2O_3—traces	$La_{0.86}Ca_{0.17}Fe_1$—93 Fe—0.11 La—3.8 Ca—0.29 Ca_1Fe_1—2.8
$La_{0.6}Ca_{0.4}FeO_{2.8}$ (0.9)	$La_{0.64}Ca_{0.39}Fe_1$	Perovskite	$La_1Ca_{0.2}Fe_1$—82.5 $Ca_{1.12}La_{0.04}Fe_1$—13 La—3.5 Ca—0.5 Fe—0.5
$La_{0.4}Ca_{0.6}FeO_{2.7}$ (1)	$La_{0.42}Ca_{0.58}Fe_1$	Perovskite $Ca_2Fe_2O_5$ Fe_2O_3—traces La_2O_3—traces	$La_{0.83}Ca_{0.17}Fe_1$—70 $Ca_1La_{0.04}Fe_1$—26.43 Fe—0.27 La—2.5 Ca—0.8
$La_{0.2}Ca_{0.8}FeO_{2.6}$ (0.5)	$La_{0.22}Ca_{0.78}Fe_1$	Perovskite $Ca_2Fe_2O_5$	$La_{0.77}Ca_{0.23}Fe_1$—39 $Ca_1La_{0.04}Fe_1$—59 Fe—0.8 La—0.56 Ca—0.64
$Ca_2Fe_2O_5$ (0.5)	$Ca_{0.98}Fe_1$	$Ca_2Fe_2O_5$	Ca_1Fe_1—96 Ca—3.2 Fe—0.8

Note: Specific notes are given in Table 1.

tion at 1100°C, the calcium content of perovskite decreased and was equal to 0.23 mole fractions. According to differential dissolution data, the main oxide phase was a Ca–Fe–O oxide phase. The formation of an anion-ordered phase with $n = 3$ was not detected by X-ray diffraction analysis (a superstructural peak with an interplanar spacing of 11.3 Å, which is characteristic of this phase, is absent; Fig. 1b, spectrum *2*) and differential dissolution.

$Ca_2Fe_2O_5$. The X-ray diffraction patterns exhibited the presence of only a brownmillerite phase. According to differential dissolution data, the stoichiometric ratio between cations in the phase is 1 : 1. The concentration of this phase was as high as 83% even after calcination at 700°C. The concentrations of parent oxides decreased with calcination temperature.

Thus, the differential dissolution data did not support the formation of a homogeneous solid solution for a composition with $x = 0.4$. Moreover, the solubility of samples allowed us to draw a conclusion regarding the disordered microstructure of the samples. The stoichiometry and phase composition of only the terminal members of the series, $LaFeO_3$ and $Ca_2Fe_2O_5$, corresponded to the expected characteristics. Intermediate compositions did not exhibit such a correspondence because double oxides were primarily formed as conglomerates at the stage of activation. A stoichiometric solid solution of a definite composition cannot be distinguished in these conglomerates even after calcination at 700°C. An increase in the calcination temperature up to 900°C resulted in the formation of homogeneous solid solutions of calcium in lanthanum ferrite. The calcium content of the solid solution increased with the calcium content of the starting mixture (Table 2). The data suggest that the particles are composites with lanthanum ferrite in the core; the next region consists of a solid solution with the calcium content decreasing to the center, and the outer layer has the stoichiometry of calcium ferrite. Thus, we believed that an increase in either the duration or the temperature of calcination makes it possible to obtain equilibrium ternary solid solutions.

However, an increase in the calcination temperature up to 1100°C did not result in the formation of homogeneous solid solutions with a stoichiometry specified in the synthesis: all intermediate samples became biphasic. In all compositions, the calcium content of perovskite was ~0.2 mole fractions, and the Ca–Fe–O oxide phase was doped with lanthanum (Table 3).

An increase in the time of calcination at 900°C up to 15 h also caused no increase in the calcium content of a solid solution. The calcium content of a solid solution increased with the calcium content of the starting mixture; however, it was no higher than 0.17 mole frac-

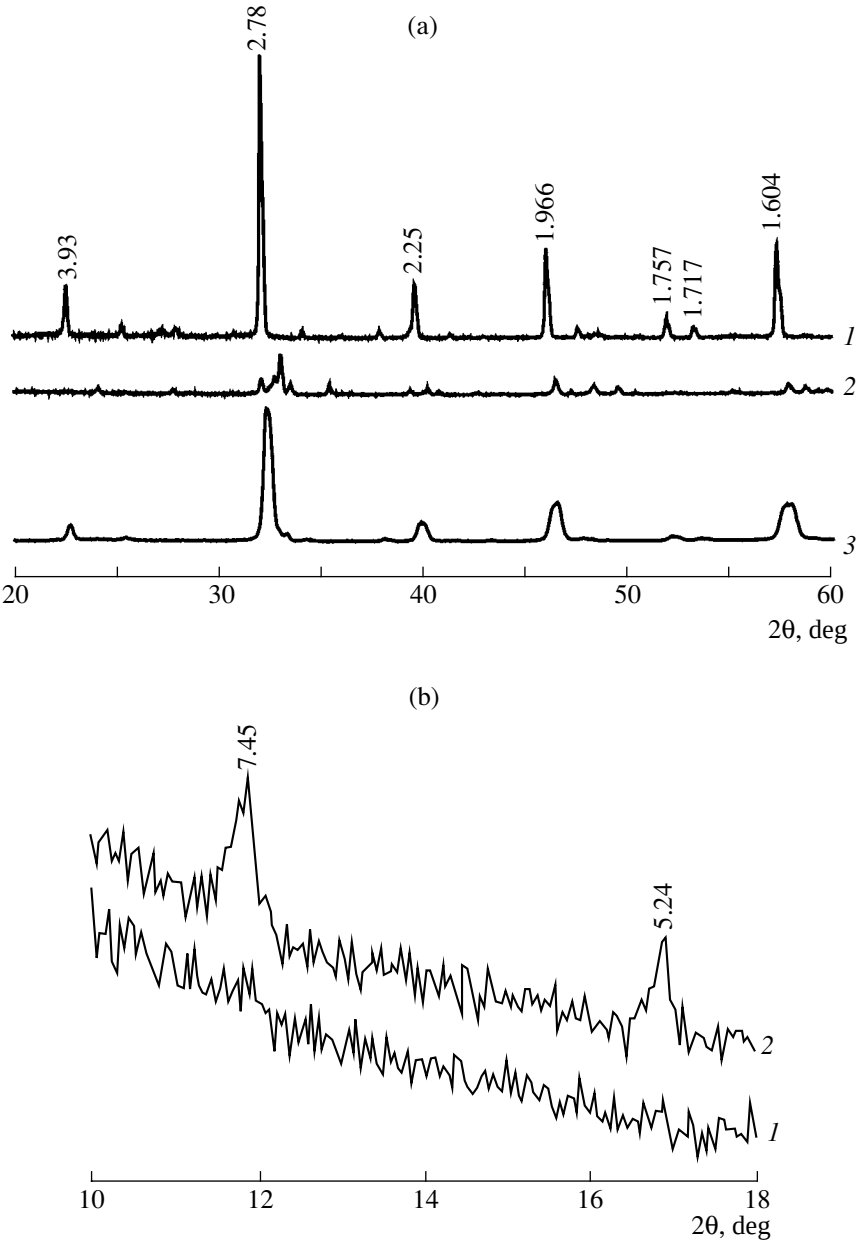

Fig. 1. X-ray diffraction patterns of samples calcined at 1100°C for 4 h: (a) (*1*) $LaFeO_3$, (*2*) $Ca_2Fe_2O_5$, and (*3*) $La_{0.6}Ca_{0.4}FeO_{2.8}$; (b) (*1*) $La_{0.6}Ca_{0.4}FeO_{2.8}$ and (*2*) $La_{0.2}Ca_{0.8}FeO_{2.6}$.

tions. These data, in combination with the previously published data on the ceramic synthesis [4], indicate that solid solutions of calcium in the structure of lanthanum ferrite with calcium contents higher than 0.2 mole fractions are unstable at room temperature.

Microstructure of Samples

A study of the samples by high-resolution electron microscopy provided support for a conclusion regarding the microstructural features of low-temperature (900°C) samples (Fig. 2a) drawn from the data of differential dissolution. The electron-microscopic data are considered below.

$La_{0.6}Ca_{0.4}FeO_{2.8}$ and $La_{0.4}Ca_{0.6}FeO_{2.7}$. The samples after calcination at 900°C consisted of coarse particles coated with a layer of irregularly stacked micrograins (Fig. 2a). Micrometer-sized particles with a disordered structure and crystallites with regular surface and bulk structures were detected as well. After calcination at 1100°C, coarse (greater than 3 μm) well-crystallized particles of two types with the structures of perovskite and brownmillerite were detected in the samples (Fig. 2b). A similar particle microstructure was also observed in a $La_{0.4}Ca_{0.6}Fe_{2.7}$ sample.

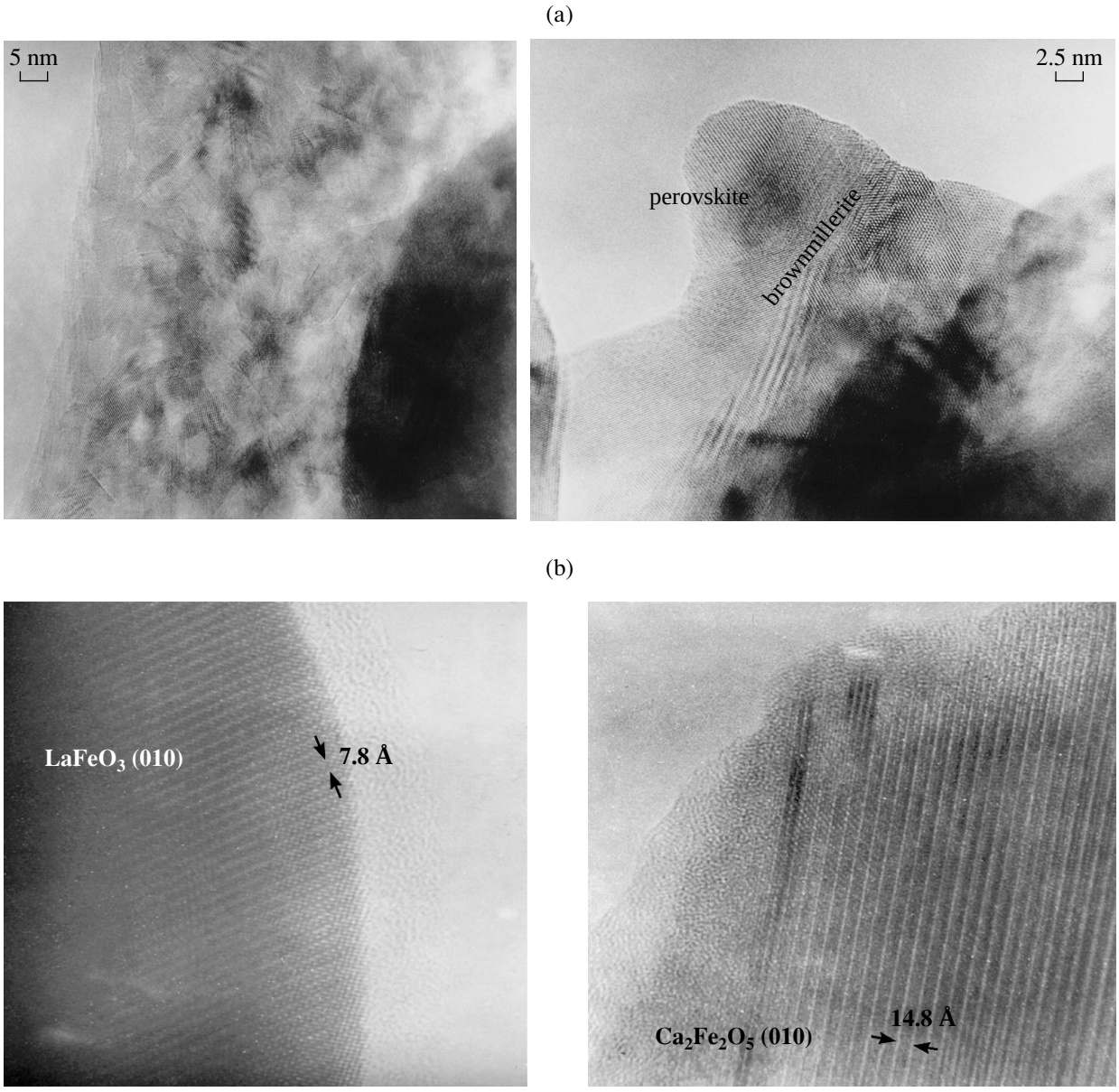

Fig. 2. Typical particle shapes of the $La_{0.6}Ca_{0.4}FeO_{2.8}$ sample prepared with the use of mechanochemical activation and calcined at (a) 900 or (b) 1100°C for 4 h.

$La_{0.2}Ca_{0.8}FeO_{2.6}$. A characteristic feature of the sample calcined at 700°C was the occurrence of a disordered layer on the surface of coarse (greater than 1.5 μm) particles with a remarkably well crystallized structure. The coating was nonuniform, and the thickness varied from 300 to 1200 Å. Particles with a large number of microtwins were also observed. The presence of medium-sized particles (0.2 μm) with a structure disordered on the atomic level was also detected. Thus, indeed, the sample consisted of a mixture of two phases, and the disordered structure of particles of these phases may be responsible for the similarity of their dissolution conditions. The disordered surface layer was not detected after calcination at 900°C; the surface of coarse particles became remarkably regular, and their bulk structure became further improved.

Tables 1–3 summarize the results of measurements of the specific surface areas of oxides prepared under different conditions. These data indicate that the specific surface area of samples of a particular composition decreased with calcination temperature. An increase in the calcium content of oxides resulted in a decrease in the specific surface area of the oxides, all other factors being the same.

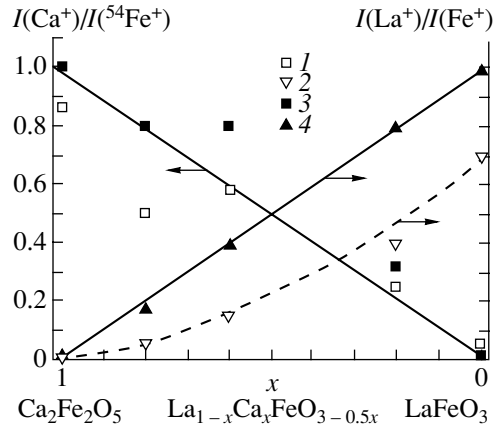

Fig. 3. SIMS data on the (*1*, *2*) surface and (*3*, *4*) bulk chemical composition of samples calcined at 900°C.

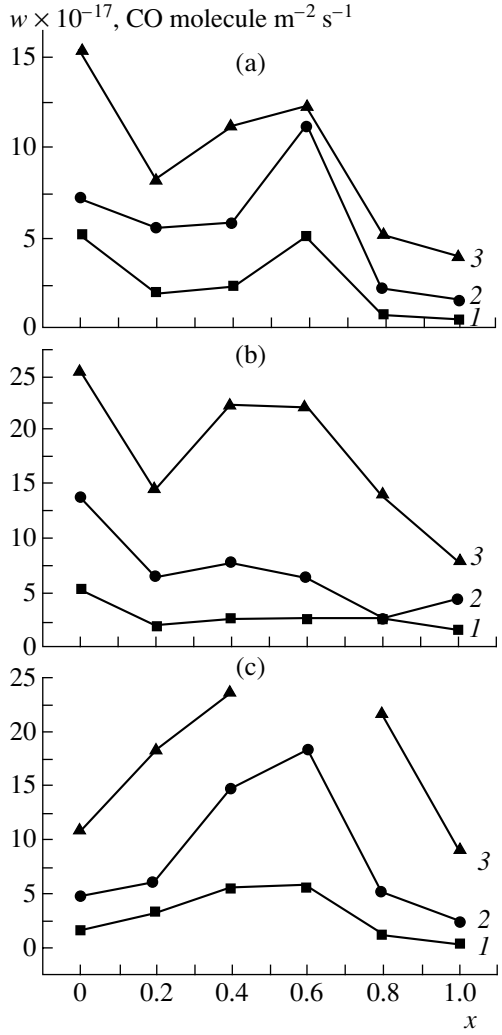

Fig. 4. Effect of the chemical composition (x in $La_{1-x}Ca_xFeO_{3-0.5x}$) on the catalytic properties of perovskites calcined at (a) 700, (b) 900, and (c) 1100°C. Test temperatures, °C: (*1*) 400, (*2*) 450, and (*3*) 500.

Surface and Bulk Composition of Samples

A SIMS study of the sample composition (Fig. 3) demonstrated that the $^{56}Ca/^{54}Fe$ ratio between ion currents both in the bulk and at the surface was symbatic to the chemical composition. The La/Fe ratio between ion currents in the bulk was also symbatic to the chemical composition. Depletion of the surface in lanthanum was observed in the samples calcined at 900°C; this fact confirms the previous conclusion, which was drawn from solubility data, regarding the surface enrichment of these samples in calcium ferrite. The O/Fe ratio between ion currents was independent of x for the samples calcined at 1100°C. It should also be noted that this ratio at the surface was higher than that in the bulk; this fact indicates that the surface was enriched in oxygen. The above ratios were equal for the surface and the bulk in the samples calcined at 900°C. Thus, the SIMS data suggest that the concentrations of iron cations at the surface were equal in all samples, whereas the surface of the samples calcined at 1100°C was enriched in oxygen.

Catalytic Activity

At all calcination temperatures, the catalytic activity of perovskites from this series in carbon monoxide oxidation changed nonmonotonically as the calcium content was increased. As in the ceramic series, an activity maximum was detected at a composition of $x = 0.4$–0.6 (Fig. 4); this maximum is not associated with an increase in the surface concentration of iron cations. The occurrence of an activity maximum in the samples calcined at 900°C does not correlate with the calcium content of the resulting nonequilibrium microheterogeneous solid solutions. As in the case of the ceramic series, this maximum can be due to a maximum density of interphase boundaries for intermediate compositions, because the samples are biphasic. According to electron-microscopic analysis, the samples exhibit a disordered structure; according to the SAXS data given below, a maximum density of these boundaries was detected in these samples. Clustered reduced centers of adsorption and catalysis can be formed at the outlets of these boundaries [13]; these centers are capable of adsorbing weakly bound oxygen. The increase in the catalytic activity of calcium-containing samples as the calcination temperature was increased up to 1100°C (Fig. 5) can be explained, for example, by the removal of residual anions and by the crystallization of disordered surface regions (i.e., an improvement in the crystal structure of lanthanum ferrite and calcium ferrite phases) [10].

Small-Angle X-ray Scattering

All of the samples exhibited small-angle scattering from the regions with altered electron density with a size of ~40 Å. This size is comparable to the sizes of X-ray amorphous particles or grain boundaries. Indeed,

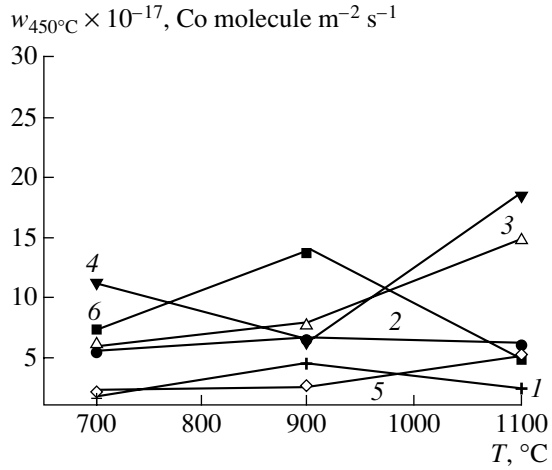

Fig. 5. Specific catalytic activities (test temperature of 450°C) of chemically different samples as functions of calcination temperature: (*1*) $Ca_2Fe_2O_5$, (*2*) $La_{0.8}Ca_{0.2}FeO_{2.9}$, (*3*) $La_{0.6}Ca_{0.4}FeO_{2.8}$, (*4*) $La_{0.4}Ca_{0.6}FeO_{2.7}$, (*5*) $La_{0.2}Ca_{0.8}FeO_{2.6}$, and (*6*) $LaFeO_3$.

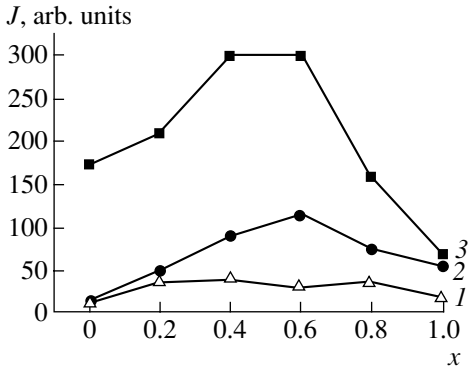

Fig. 6. Integrated SAXS intensity as a function of the chemical composition (x in $La_{1-x}Ca_xFeO_{3-0.5x}$) at the following sample calcination temperatures: (*1*) 1100, (*2*) 900, and (*3*) 700°C.

the dependence of the SAXS intensity on the chemical composition of samples or on the calcination temperature (Fig. 6) exhibits a maximum at an intermediate composition, and it is symbatic to the dependence of the specific catalytic activity on the sample composition. The occurrence of a maximum may correspond to a higher density of interphase boundaries in samples with intermediate compositions. It is likely that a decrease in the number of these regions with calcination temperature results from the degradation of a microheterogeneous solid solution, as well as the processes of crystallization and sintering.

Thus, we found that the substitution of calcium for lanthanum in lanthanum ferrite in the synthesis performed using mechanochemical activation did not result in the formation of a continuous series of homogeneous solid solutions based on a perovskite structure. We also found that a limited series of solid solutions with calcium content no higher than 0.5 mole fractions can be formed under nonequilibrium conditions. The resulting solid solutions are nonequilibrium because the calcium content of the samples decreased with the time or temperature of calcination. As in the ceramic series, a maximum equilibrium calcium content in the perovskite structure was no higher than 0.2 mole fractions.

According to definition [14], intermediate samples from the test series, which are disordered microheterogeneous solid solutions, can be categorized as nanophase materials even after calcination at 900°C.

Samples from this series with medium compositions exhibited the highest catalytic activity. The observed change in the specific catalytic activity correlates with the maximum density of interphase boundaries for these samples (because it is believed that the samples of intermediate composition in a two-phase system exhibit the maximum density of interphase boundaries) and with a change in the relative density of regions with altered electron density (according to SAXS data), in particular, related to interphase boundaries. It is likely that the specific catalytic activity increased with the temperature of calcination because of the crystallization of disordered regions.

Thus, the synthesis of perovskites from the La–Ca–Fe–O series with the use of mechanochemical activation does not result in the formation of a continuous series of homogeneous solid solutions. In this case, we did not detect the formation of a vacancy-ordered Grenier phase. A special feature of the microstructure of low-temperature (700–900°C) are the randomly stacked regions with the perovskite and brownmillerite structures within a particle, which result in the formation of a high density of interphase boundaries.

ACKNOWLEDGMENTS

This study was supported by the Russian Foundation for basic Research (project no. 99-03-32836).

REFERENCES

1. Yamazoe, V. and Teraoka, J., *Catal. Today*, 1990, vol. 8, p. 175.
2. Grenier, J.C., Fournes, L., Pouchard, M., Hagenmuller, P., and Komorniski, S., *Mater. Res. Bull.*, 1982, vol. 17, p. 55.
3. Wu, Y., Yu, T., Dou, B., and Wang, C., *J. Catal.*, 1989, vol. 120, p. 88.
4. Isupova, L.A., Yakovleva, I.S., Tsybulya, S.V., Kryukova, G.N., Boldyreva, N.N., Vlasov, A.A., Alikina, G.M., Ivanov, V.P., and Sadykov, V.A., *Kinet. Katal.*, 2000, vol. 41, no. 2, p. 315.
5. Rao, C.N.R., Gopalakrishnan, J., and Vidyasagar, K., *Indian J. Chem.*, 1984, vol. 23A, p. 265.

6. Isupova, L.A. and Tsybylya, S.V., Kryukova, G.N., Boldyreva, N.N., Alikina, G.M., Ivanov, V.P., and Sadykov, V.A., *ECSSC'99*, Madrid, 1999, vol. 1, p. O4.
7. Tret'yakov, Yu.D. and Gudilin, E.A., *Usp. Khim.*, 2000, vol. 69, no. 1, p. 3.
8. Isupova, L.A., Sadykov, V.A., Avvakumov, E.G., and Kosova, N.V., *Chemistry in Sustainable Development*, Cambridge, 1998, vol. 6, nos. 1–2, p. 207.
9. Kosova, N.V., Devyatkina, E.T., Avvakumov, E.G., Gainutdinov, I.I., Rogachev, A.Yu., Pavlyukhin, Yu.T., Isupova, L.A., and Sadykov, V.A., *Inorg. Mater.*, 1998, vol. 34, no. 4, p. 478.
10. Isupova, L.A., Tsybulya, S.V., Kryukova, G.N., Ivanov, V.P., Paukshtis, E.A., Budneva, A.A., Boldyreva, N.N., and Sadykov, V.A., *Abstr. 6th Eur. Conf. on Solid State Chem.*, Zurich, 1997, vol. 2, p. PB81.
11. Malakhov, V.A. and Vlasov, A.A., *Kinet. Katal.*, 1995, vol. 36, no. 4, p. 503.
12. Sadykov, V.A., Tikhov, S.F., and Kryukova, G.N., *J. Solid State Chem.*, 1988, vol. 74, p. 200.
13. Sadykov, V.A., Tikhov, S.F., Tsybulya, S.V., *et al.*, *Stud. Surf. Sci. Catal.*, 1997, vol. 110, p. 1155.
14. Ivanov, Yu.F., Lopatin, V.V., and Dedkov, V.S., *Izv. Vyssh. Uchebn. Zaved., Fiz.*, 1994, vol. 1, p. 107.